The Cytoskeleton in the Extraocular Muscles of Desmin Knockout Mice

Maria Angels Rodríguez,[1] Jing-Xia Liu,[2] Kimmo Parkkonen,[1,2] Zhenlin Li,[3] and Fatima Pedrosa Domellöf[1]

[1]Department of Clinical Sciences, Ophthalmology, Umeå University, Umeå, Sweden
[2]Department of Integrative Medical Biology, Section for Anatomy, Umeå University, Umeå, Sweden
[3]Sorbonne Université, Paris, France

Correspondence: Fatima Pedrosa Domellöf, Department of Clinical Sciences, Ophthalmology, Umeå University, Umeå 901 85, Sweden; fatima.pedrosa-domellof@umu.se.

Submitted: April 5, 2018
Accepted: August 15, 2018

Citation: Rodríguez MA, Liu J-X, Parkkonen K, Li Z, Pedrosa Domellöf F. The cytoskeleton in the extraocular muscles of desmin knockout mice. *Invest Ophthalmol Vis Sci*. 2018;59:4847–4855. https://doi.org/10.1167/iovs.18-24508

Purpose. To investigate the effect of absence of desmin on the extraocular muscles (EOMs) with focus on the structure and composition of the cytoskeleton.

Methods. The distribution of synemin, syncoilin, plectin, nestin, and dystrophin was evaluated on cross and longitudinal sections of EOMs and limb muscles from 1-year-old desmin knockout mice (desmin$^{-/-}$) by immunofluorescence. General morphology was evaluated with hematoxylin and eosin while mitochondrial content and distribution were evaluated by succinate dehydrogenase (SDH) and modified Gomori trichrome stainings.

Results. The muscle fibers of the EOMs in desmin$^{-/-}$ mice were remarkably well preserved in contrast to those in the severely affected soleus and the slightly affected gastrocnemius muscles. There were no signs of muscular pathology in the EOMs and all cytoskeletal proteins studied showed a correct location at sarcolemma and Z-discs. However, an increase of SDH staining and mitochondrial aggregates under the sarcolemma was detected.

Conclusions. The structure of the EOMs was well preserved in the absence of desmin. We suggest that desmin is not necessary for correct synemin, syncoilin, plectin, and dystrophin location on the cytoskeleton of EOMs. However, it is needed to maintain an appropriate mitochondrial distribution in both EOMs and limb muscles.

Keywords: extraocular muscles, knockout, desmin, cytoskeleton, intermediate filament

Extraocular muscles (EOMs) are responsible for the complex voluntary and reflex movements of the eye, which involve a high demand of activity. The EOMs are classified as a separate muscle allotype given their unique structural and functional properties and gene expression profile.[1,2]

Several studies performed on patients and animal models of muscular dystrophy and neuromuscular disorders, such as Duchenne muscular dystrophy,[3,4] congenital muscular dystrophy with absence of laminin alpha 2 chain,[5] and amyotrophic lateral sclerosis,[6] reveal that the EOMs are selectively spared, in contrast to the limb muscles. However, data on the EOMs in desminopathies are lacking.

Desminopathies are a heterogeneous group of progressive myopathies and cardiomyopathies caused by mutations on desmin (*DES*) or αB-crystallin (*CRYAB*) genes and characterized by the presence of desmin protein aggregates and functional and structural alterations of the cytoskeleton network that lead to muscle fiber degeneration.[7] Although the disease phenotype is very heterogeneous and the first symptoms can appear at any time during the patient's lifetime, these are predominantly characterized by distal and proximal skeletal muscular weakness that coexists with cardiac pathology in half of the patients.[7,8]

Desmin is a 53-kilodalton (kDa) intermediate filament (IF) protein encoded by a single-copy gene.[9] Desmin is the most abundant cytoskeletal protein in mature muscle and for many years it was considered ubiquitous in smooth, cardiac, and skeletal muscle. However, recent work from our laboratory demonstrated that a subgroup of fibers from adult and fetal EOMs lack or express only trace amounts of desmin.[10] Notably, desmin is not required for proper muscle fiber development.[11,12]

The main function of desmin is to maintain muscle fiber cytoarchitecture by mediating the link between peripheral myofibrils and sarcolemma, nuclei, and mitochondria.[13] Desmin also links adjacent myofibrils at the Z-disc level and is enriched in myotendinous junctions (MTJs), neuromuscular junctions (NMJs), and costameres. The correct positioning and interaction of these cell compartments and organelles are critical to preserve mechanical and signaling processes taking place in the muscle in response to different stimuli.[14,15] Desmin performs its role by binding several molecules including other IF proteins and IF linker proteins. Two IF proteins that bind to desmin are synemin and syncoilin. Synemin can directly form heteropolymers with desmin,[16] whereas syncoilin can associate with desmin but without heteropolymer network formation.[17] Both proteins colocalize with desmin at the Z-discs, costameres, and myotendinous and neuromuscular junctions.[17–19,20] Nestin and vimentin are two additional IF proteins coexpressed with desmin during skeletal muscle development. In contrast to synemin and syncoilin, nestin and vimentin are downregulated postnatally in healthy skeletal muscle, with vimentin disappearing completely, whereas nestin expression in adult muscle is restricted to NMJs and MTJs[21,22] and regenerating muscle fibers.[23] We have previously shown that nestin is normally present in some muscle fibers in the adult human EOMs.[10]

Table. Antibodies Used

Antigen	Host	Supplier (Catalog No.)
Synemin H, high molecular weight	Rabbit pAb	Provided by Zhenlin Li, Sorbonne Université
Synemin H/M, high and medium molecular weight	Rabbit pAb	Provided by Zhenlin Li, Sorbonne Université
Plectin	Guinea pig pAb	Progen, Heidelberg, Germany (GP21)
Syncoilin	Rabbit pAb	Proteintech, Chicago, IL, USA (25151-1-AP)
Nestin	Mouse mAb	R&D systems, Minneapolis, MN, USA (2736)
Vimentin	Mouse mAb	Dako Omnis, Agilent, Santa Clara, CA, USA (M0725)
Dystrophin	Rabbit pAb	Gene Tex, Inc., Irvine, CA, USA (GTX15277)
MyHC IIa	Mouse mAb	Developmental Studies Hybridoma Bank, Iowa City, IA, USA (SC-71)
MyHCIIb	Mouse mAb	Developmental Studies Hybridoma Bank (BF-F3)
MyCH I	Mouse mAb	Developmental Studies Hybridoma Bank (BA-D5)
Laminin	Rabbit pAb	Dako Omnis (Z0097)

pAb, polyclonal antibody; mAb, monoclonal antibody.

In desmin knockout (desmin$^{-/-}$) mouse models, important structural modifications including muscle fiber disorganization, fibrosis, subsarcolemmal aggregation of mitochondria, and coexistence of muscle fiber regeneration and degeneration are present, particularly in the highly used muscles, such as the soleus muscle.[11,24,25] In particular, the lack of desmin produces alterations in mitochondrial distribution in soleus, gastrocnemius, and cardiac muscles.[24,26] The correct positioning of mitochondria depends on desmin interaction with plectin,[27] a major cytoskeleton cross-linking protein not included in the IF family. Important changes in desmin-binding protein patterns comprising alterations in synemin and syncoilin have been reported in the soleus muscles from desmin$^{-/-}$ mice. In the absence of desmin, both proteins are lost from the muscle fiber Z-discs, whereas their expression at the subsarcolemma is partly affected.[19,28] Moreover, in patients with desminopathy, the proteins synemin,[29] syncoilin,[7] and plectin[30] were found to colocalize with desmin aggregates.

In the present study we used a desmin$^{-/-}$ mouse model[11] to investigate the effect of absence of desmin in the structure and composition of the cytoskeleton of the EOMs. The study included the important desmin-binding proteins synemin, syncoilin, plectin, vimentin, and nestin and evaluation of the distribution of mitochondria in the desmin$^{-/-}$ EOMs, since alterations in mitochondrial network have been described in skeletal and cardiac muscle of mice lacking desmin and in patients with desminopathy.[7,25,31]

Materials and Methods

Muscle Samples

This animal study was conducted in accordance with the European Communities' Council directive (86/609/EEC), complied with the ARVO Statement for the Use of Animals in Ophthalmic and Vision Research, and had the approval of the Umeå animal experiment ethics board.

Desmin$^{-/-}$ homozygous mutant mice generated as previously described[11] were used in this study. The genotype of mice was verified by PCR of DNA from the tail with primers Des1 (5′-agaaggtgcgcttcttggag-3′), Des2 (5′-tcacttggcctt gagcctct-3′), and LacZ430R (5′-ggatcgatctcgccatacagcg-3′), which give rise to 213- and 345-bp (base pair) fragments for wild-type (WT) and desmin knockout alleles, respectively. Desmin$^{-/-}$ and age-matched control mice were killed at 1 year of age by cervical dislocation. A total of 25 EOM and 16 skeletal muscle samples comprising both the soleus and the gastrocnemius muscles from 11 desmin$^{-/-}$ mice and 8 control mice were dissected and mounted on cardboard, frozen in propane chilled in liquid nitrogen, and stored at –80°C until used. Consecutive serial cross and longitudinal sections (5–6 μm thick) were cut at –24°C with a Reichert Jung cryostat (Leica, Heidelberg, Germany).

Histochemistry

Frozen cross sections were stained with hematoxylin and eosin (H&E).[32] In addition, we used a standard protocol[32] to reveal the mitochondrial marker enzyme succinate dehydrogenase (SDH), and the modified Gomori trichrome staining was carried out as described[32] to demonstrate mitochondrial abnormalities in the EOMs.

Immunofluorescence

All sections used for immunofluorescence were air dried for 15 minutes and fixed in 4% paraformaldehyde (PFA) for 8 minutes, except for the immunodetection of myosin heavy chain (MyHC) isoforms, where no fixation was performed. Thereafter, the sections were washed in PBS and blocked with 10% normal serum (from goat or donkey depending on the host species of the secondary antibody used) in PBS containing 1% Tween, for 15 minutes. Immediately after blocking, sections were incubated overnight (O/N) with the primary antibody (Table) diluted in PBS with 10% normal serum at 4°C. After washing with PBS, sections were incubated at 4°C for 3 hours with a species-specific secondary antibody conjugated with Alexa Fluor (Jackson ImmunoResearch, West Grove, PA, USA), diluted in PBS with 10% normal serum. Subsequently, the slices were washed in PBS and coverslips were mounted with Vectashield mounting medium (Vector Laboratories, Inc., Burlingame, CA, USA).

For NMJ detection, sections were incubated with alpha-bungarotoxin Alexa Fluor 594–conjugated (Molecular Probes, Inc., Eugene, OR, USA) for 1 hour at room temperature (RT), washed in PBS, and mounted with Vectashield medium.

Antibodies against different MyHC isoforms were combined with primary antibody against laminin in order to count the number of muscle fibers containing the different MyHC isoforms per total number of muscle fibers in each preparation. For double and triple immunostaining, a cocktail of primary and subsequently secondary antibodies was used. When the combination of primary antibodies was not possible, the sections were processed as described above for the first primary and secondary antibody and the next day, after washing in PBS and an additional blocking with 5% normal serum for 15 minutes, sections were incubated O/N at 4°C with the second primary antibody and the protocol continued as usual.

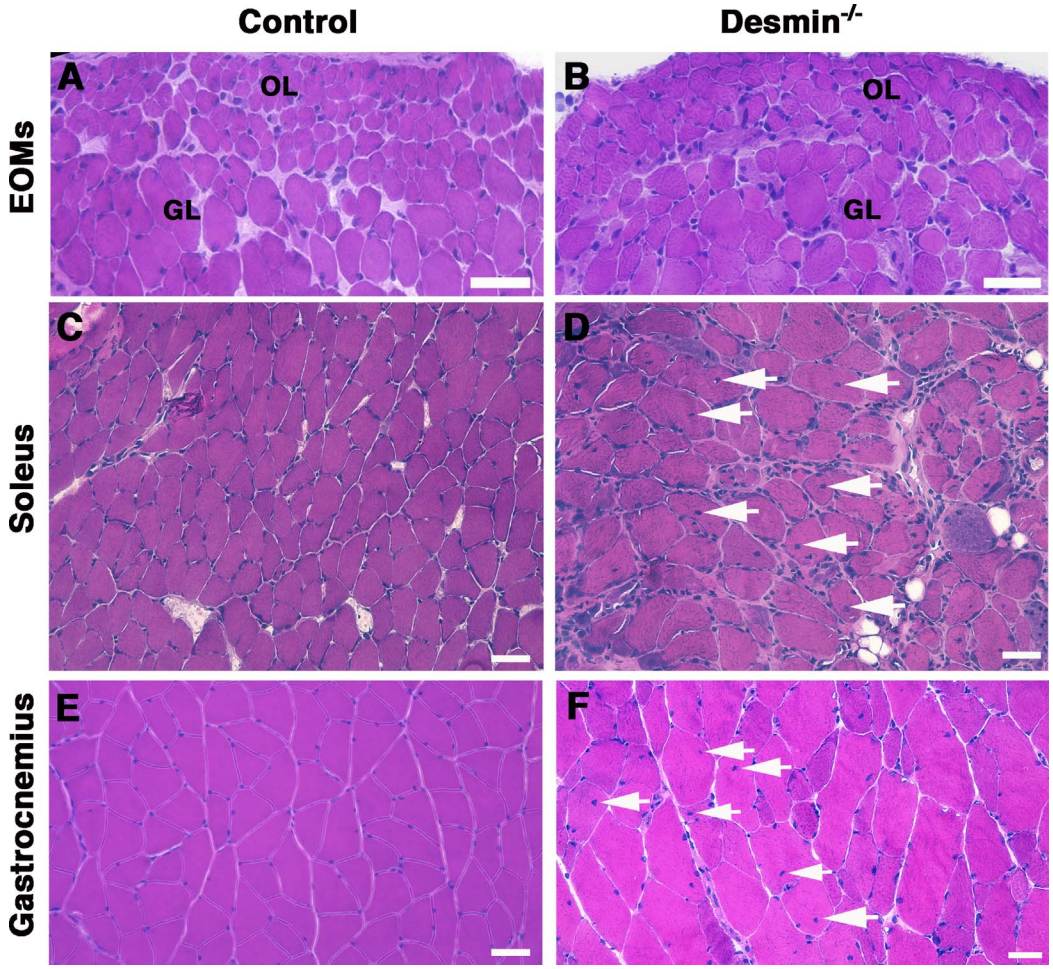

FIGURE 1. Cross sections of EOMs (**A**, **B**), soleus (**C**, **D**), and gastrocnemius muscles (**E**, **F**) from 1-year-old control (**A**, **C**, **E**) and desmin$^{-/-}$ mice (**B**, **D**, **F**) stained with hematoxylin and eosin (H&E). Desmin$^{-/-}$ EOMs showed preserved architecture in both orbital (OL) and global layers (GL) (**B**), whereas the desmin$^{-/-}$ soleus muscle showed clear pathological signs (**D**) including increased connective tissue, central myonuclei (*arrows*), and higher variability of muscle fiber size (**D**). The morphology of the gastrocnemius muscles (**F**) was more preserved than that of the soleus muscle on desmin$^{-/-}$ samples, but higher variability of muscle fiber size and muscle fibers with central nuclei (*arrows*) was also present. *Scale bars*: 40 µm.

Negative controls were processed as above, but the primary antibody was omitted. No immunolabeling was detected in control sections.

Images were taken with a Spot camera (RT KE slider; Diagnostic Instruments, Inc., Sterling Heights, MI, USA) connected to a Nikon microscope (Eclipse, E800; Tokyo, Japan) or with a digital high-speed fluorescence CCD camera (Leica DFC360 FX) connected to a Leica microscope (Leica DM6000B; Leica Microsystems CMC, GmbH, Wetzlar, Germany). Images were processed using Adobe Photoshop software (Adobe Systems, Inc., Mountain View, CA, USA) and Fiji image processor.[33]

Statistical Analysis

The percentage of centrally nucleated fibers (CNFs) was calculated in cross-sectioned EOMs from six desmin$^{-/-}$ mice and five control mice stained with H&E.

Muscle fiber size was determined by measuring the cross-sectional area of a total of 5338 muscle fibers, from 11 desmin$^{-/-}$ mice and 8 control mice, immunolabeled against dystrophin and using Qwin software (Leica Microsystems Ltd., Heerbrugg, Switzerland) in orbital and global layers. The area of each muscle fiber was determined and averaged per layer and per animal.

All data are presented as mean values ± standard error of the mean (SEM). Statistical differences between the two animal groups for centrally CNFs, fiber size, and percentage of muscle fibers containing different MyHC isoforms were assessed by unpaired *t*-test. $P < 0.05$ was considered statistically significant.

RESULTS

Morphology

The histologic profile of the control and desmin$^{-/-}$ EOMs, assessed in H&E sections, was characterized by round muscle fibers of variable size with smaller diameter on the orbital layer and larger diameter on the global layer (Figs. 1A, 1B). Muscle fibers in desmin$^{-/-}$ EOMs showed preserved morphology with no detectable differences when compared to control samples, even at very high magnification. Muscle fiber size was determined in both orbital and global layers and revealed no statistically significant differences when compared to control EOMs, neither in the orbital layer ($P = 0.38$) nor the global ($P = 0.56$) layer. Desmin$^{-/-}$ EOMs lacked signs of muscular pathology (Fig. 1B). In particular, no visible increase in connective tissue or adipose tissue and no signs of inflamma-

tion or atrophy could be seen. The presence of central nuclei in the myofibers of the EOMs was rare and very similar in both the controls and the desmin$^{-/-}$ mice (0.36% ± 0.05 in controls and 0.94% ± 0.41 in desmin$^{-/-}$, $P = 0.23$). In contrast, the soleus muscle appeared visibly affected in desmin$^{-/-}$ mice, as previously reported,[24] with an increase of connective tissue, evident fiber size variability, and fibers containing central nuclei (Fig. 1D) and with signs of fiber splitting (Supplementary Fig. S1A). When compared to the EOMs, which showed a preserved morphology, and to the soleus muscle that is broadly affected, muscle fibers in the gastrocnemius muscle showed intermediately affected morphology, characterized by apparent larger variation in fiber size, occasional muscle fibers containing central nuclei, and some fiber splitting, but these were less common than in the soleus muscles, as previously described[24] (Fig. 1F; Supplementary Fig. S1B).

A characterization of the content of different MyHC isoforms in the midbelly region of the EOMs from four desmin$^{-/-}$ and four control mice was performed. The percentage of fast fibers in the EOMs was analyzed by immunodetection of muscle fibers labeled with antibodies against MyHC fast IIa (MyHCIIa) and MyHC fast IIb (MyHCIIb). Muscle fibers containing MyHCIIx could not be studied because of the lack of a specific antibody that would work in the EOMs, where all myofibers contain more than a single MyHC isoform. The percentage of muscle fibers containing fast MyHC isoforms (MyHCIIa or MyHCIIb) was 21.47% ± 2.16 and 18.85% ± 2.65 in the EOMs of controls and desmin$^{-/-}$, respectively ($P = 0.47$). The amount of muscle fibers containing MyHCI showed a tendency to increase from 8.32% ± 1.92 in controls to 14.77% ± 1.98 in desmin$^{-/-}$ EOMs ($P = 0.06$).

In sections treated to show the activity of the mitochondrial enzyme SDH in control EOMs, a checkerboard staining pattern was present, characterized by a combination of different staining intensities between muscle fibers, indicating different levels of oxidative capacity. At the subcellular level, SDH staining showed a fine to coarse granular appearance (Fig. 2A). In desmin$^{-/-}$ EOMs this pattern was conserved inside muscle fibers. However, in addition, subsarcolemmal aggregations with a darker SDH staining (Fig. 2B) appeared in 57% of the mice analyzed and independently of the EOM layer analyzed. In addition, a Gomori trichrome staining was performed in order to better characterize the mitochondrial distribution inside the muscle fibers at higher magnification. In the orbital layer of desmin$^{-/-}$ and control EOMs, the muscle fibers were small, mostly darkly stained, and displayed abundant mitochondria that could be observed in red, both in the periphery and inside of the muscle fibers (Figs. 3A, 3B). In the global layer, fiber size and content of mitochondria were more heterogeneous, with the presence of darkly and lightly stained fibers in both desmin$^{-/-}$ and control EOMs (Figs. 3C, 3D). Notably, desmin$^{-/-}$ EOMs contained a very small percentage (approximately 3%) of muscle fibers in the global layer, with mitochondrial accumulations present mostly at the periphery of the muscle fibers (Fig. 3D).

As previously reported,[26] alterations of mitochondrial distribution in desmin$^{-/-}$ mice were seen in the soleus and gastrocnemius muscles, being notably more abundant in the fibers of the soleus muscle (Fig. 2D). The characteristic checkerboard pattern was lost in the soleus of desmin$^{-/-}$ mice and subsarcolemmal SDH staining accumulations appeared, accompanied by reduced staining in the sarcoplasmic area (Fig. 2D). The SDH staining pattern of gastrocnemius muscle of desmin$^{-/-}$ mice (Fig. 2F) was predominantly similar to that of the control gastrocnemius muscles. However, approximately 30% to 40% of the muscle fibers located in the deep part of the muscle, an area containing both slow and fast muscle fibers, showed abnormal accumulations of mitochondria, as previously reported.[26]

Distribution of Desmin-Binding Proteins

In cross-sectioned control EOM samples, both synemin and syncoilin (Figs. 4A, 4B) were present beneath the sarcolemma and there was a mild sarcoplasmic immunostaining characterized by either a punctated pattern for syncoilin (Fig. 4B) or a combination of punctated and homogeneous pattern for synemin (Fig. 4A). Plectin labeling appeared in the subsarcolemmal region and was slightly weaker in the sarcoplasma (Fig. 4C). For all three proteins, staining patterns were indistinguishable between the global layer and the orbital layer, although different staining intensities were noted among muscle fibers in a given muscle section, independently of muscle layer. In longitudinal sections, synemin, syncoilin, and plectin presented a cross-striated staining pattern corresponding to the fiber Z-discs (Figs. 4D–F).

In cross-sectioned desmin$^{-/-}$ EOMs (Figs. 4G–I), no obvious changes in the immunostaining patterns for synemin, syncoilin, or plectin were noted when compared to control EOMs. The heterogeneity in immunostaining patterns for all three proteins between fibers described above for the EOMs of control mice was also noted in the desmin$^{-/-}$ EOMs. Additionally, in longitudinal sections the immunostaining patterns of synemin, syncoilin, and plectin at Z-discs were identical to those observed in the control EOMs (Figs. 4J–L).

In contrast, desmin$^{-/-}$ soleus muscle showed synemin, syncoilin, and plectin distribution changes (Figs. 5D–F). For synemin and syncoilin, these changes were characterized by an irregular subsarcolemmal staining and numerous muscle fibers with subsarcolemmal aggregates that occasionally also coexisted with sarcoplasmic aggregates (Figs. 5D, 5E). Synemin aggregates were more prevalent than syncoilin aggregates (Figs. 5D, 5E). Plectin immunostaining in desmin$^{-/-}$ soleus muscle was in general weaker than in the controls, and its immunodetection in the subsarcolemma area appeared irregular compared to the control fibers. In addition, subsarcolemmal and, to a lesser extent, sarcoplasmic dense plectin-positive aggregates were present in sporadic muscle fibers of desmin$^{-/-}$ soleus samples (Fig. 5F). In contrast, the gastrocnemius muscle of desmin$^{-/-}$ mice (Figs. 5G–I) showed a conserved pattern for synemin, syncoilin, and plectin distribution comparable to control gastrocnemius, and no aggregates were observed.

Nestin labeling was absent in the EOMs of both WT and desmin$^{-/-}$ mice (not shown). This finding was in contrast to desmin$^{-/-}$ soleus and gastrocnemius muscles, where moderate labeling compatible with nestin aggregates was seen in a small number of muscle fibers. The aggregates displayed a coarse appearance, and were located either centrally inside the fiber or peripherally beneath the sarcolemma in some fibers (not shown). Vimentin immunodetection was negative in the muscle fibers of the EOMs, soleus, and gastrocnemius muscles of both WT and desmin$^{-/-}$ mice (not shown).

The antibody against dystrophin uniformly labeled the subsarcolemma contours of the muscle fibers in both control and desmin$^{-/-}$ EOMs (Fig. 6). In contrast, although labeling against dystrophin in desmin$^{-/-}$ soleus and gastrocnemius muscle generally showed a homogeneous subsarcolemmal pattern, some accumulations of dystrophin beneath the sarcolemma of soleus, but not gastrocnemius, muscle were noted in less than 5% of the muscle fibers, together with an increased variability in fiber size and increased space between muscle fibers (Fig. 6D), in comparison to the control soleus samples (Fig. 6C).

Investigative Ophthalmology & Visual Science

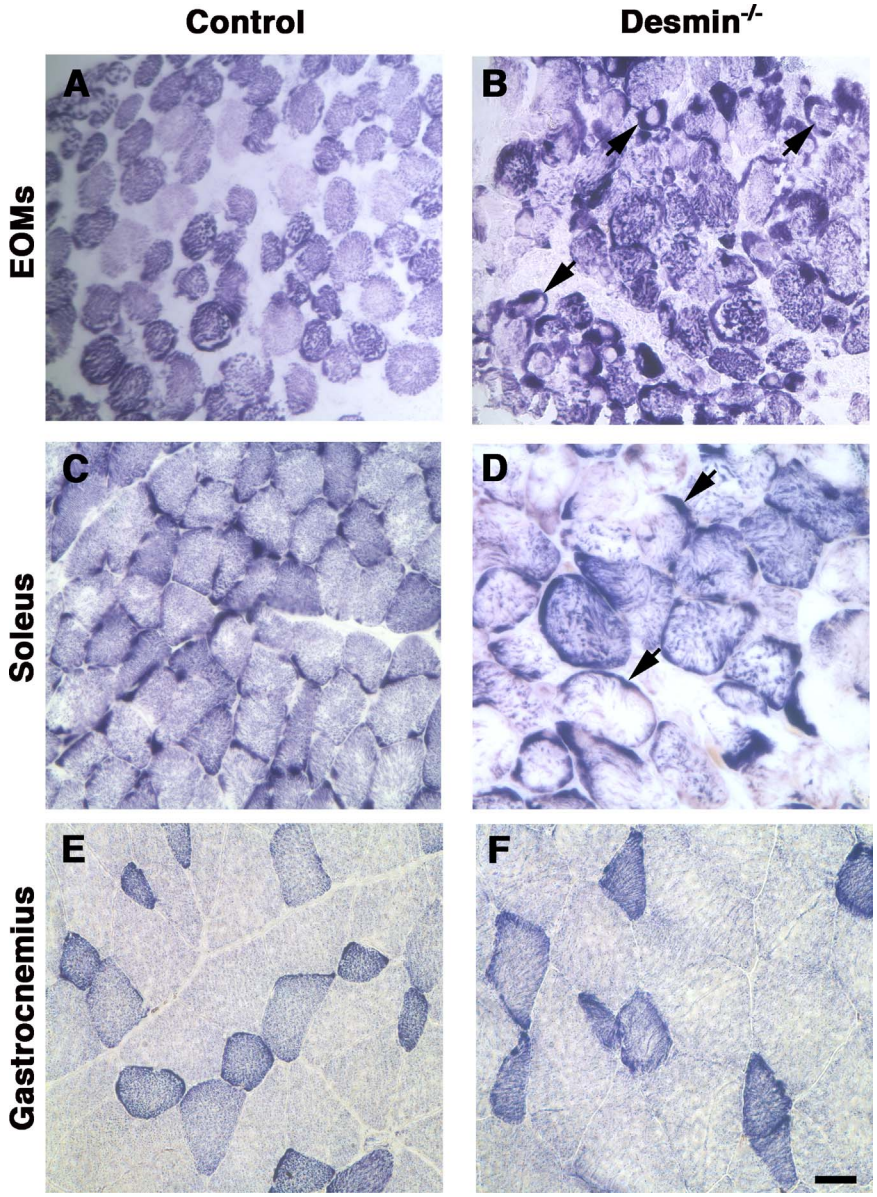

FIGURE 2. Cross sections of EOMs (**A**, **B**), soleus (**C**, **D**), and gastrocnemius (**E**, **F**) muscles from 1-year old control (**A**, **C**, **E**) and desmin$^{-/-}$ (**B**, **D**, **F**) mice were processed to demonstrate SDH activity. In EOMs from desmin$^{-/-}$ mice, SDH staining revealed subsarcolemmal mitochondria accumulation (**B**, *arrows*) with a generally stronger SDH staining in some muscle fibers. In soleus muscle of desmin$^{-/-}$ mice the normal checkerboard pattern was altered and accumulation of mitochondria appeared at the subsarcolemma level (**D**, *arrows*) whereas SDH staining intensity was reduced inside the muscle fibers. The gastrocnemius muscle conserved the checkerboard pattern for the most part of the muscle with a predominance of mildly stained fast fibers (**F**). *Scale bar*: 20 μm.

DISCUSSION

In the present study we show for the first time the effect of lack of desmin on the distribution of important proteins of the cytoskeleton in the EOMs.

For this study we used 1-year-old animals, at the end of the life span of this animal model, in order to take into account the possibility of a delayed effect of the lack of desmin in the morphology of the EOMs. Changes on limb and cardiac muscles have been described in the same animal model at the age of 3 months.[24] Here, we found that muscle fibers from EOMs of 1-year-old desmin$^{-/-}$ mice showed a preserved cytoskeletal structure at the light-microscopic level comparable to that of control EOM samples. These results differ from those on the soleus muscle, where the lack of desmin led to pathological manifestations readily visible, in agreement with previous reports.[11,24] The structure of the gastrocnemius muscle appeared broadly conserved in desmin$^{-/-}$ mice. However, pathological changes similar to those detected in the soleus muscle and including central nuclei and fiber splitting were also present, but to a milder degree, indicating that the gastrocnemius muscle is not as spared as the EOMs were in the context of lack of desmin. Our findings are in line with previous studies on other diseases such as Duchenne muscular dystrophy or amyotrophic lateral sclerosis,[3,4,6] which strongly affect limb muscles, whereas the EOMs appear selectively spared or only mildly affected. In our desmin$^{-/-}$ mouse model, although the EOMs showed a healthy morphology analyzed by H&E and confirmed with dystrophin labeling, the absence of desmin produced abnormalities in the

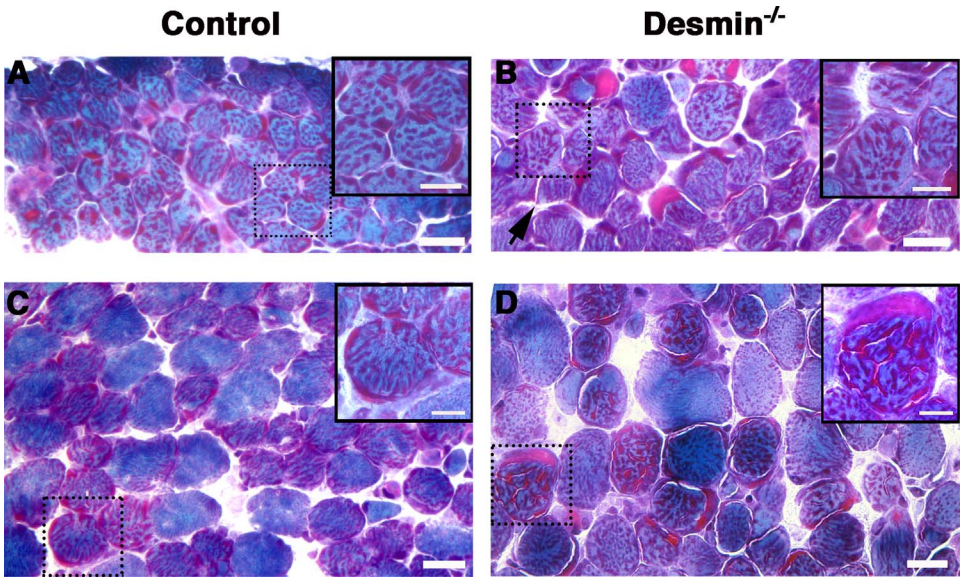

FIGURE 3. Cross sections of EOM orbital (**A**, **B**) and global layer (**C**, **D**) from 1-year old control (**A**, **C**) and desmin$^{-/-}$ mice (**B**, **D**) stained with modified Gomori trichrome. Amplified regions (*scale bar*: 10 μm) of representative muscle fibers are indicated by *dotted lines* and detailed inside the *squares on the upper right corner*. Muscle fibers in the orbital layer generally displayed a higher content of mitochondria observed in red color under the sarcolemma and in the sarcoplasma of the fibers in a similar pattern in controls and desmin$^{-/-}$ animals (**A**, **B**). In the global layer different patterns of mitochondrial content among muscle fibers were observed (**C**, **D**), and in the desmin$^{-/-}$ mice subsarcolemmal accumulations were present in some muscle fibers (**D**, *square*). *Scale bar*: 20 μm.

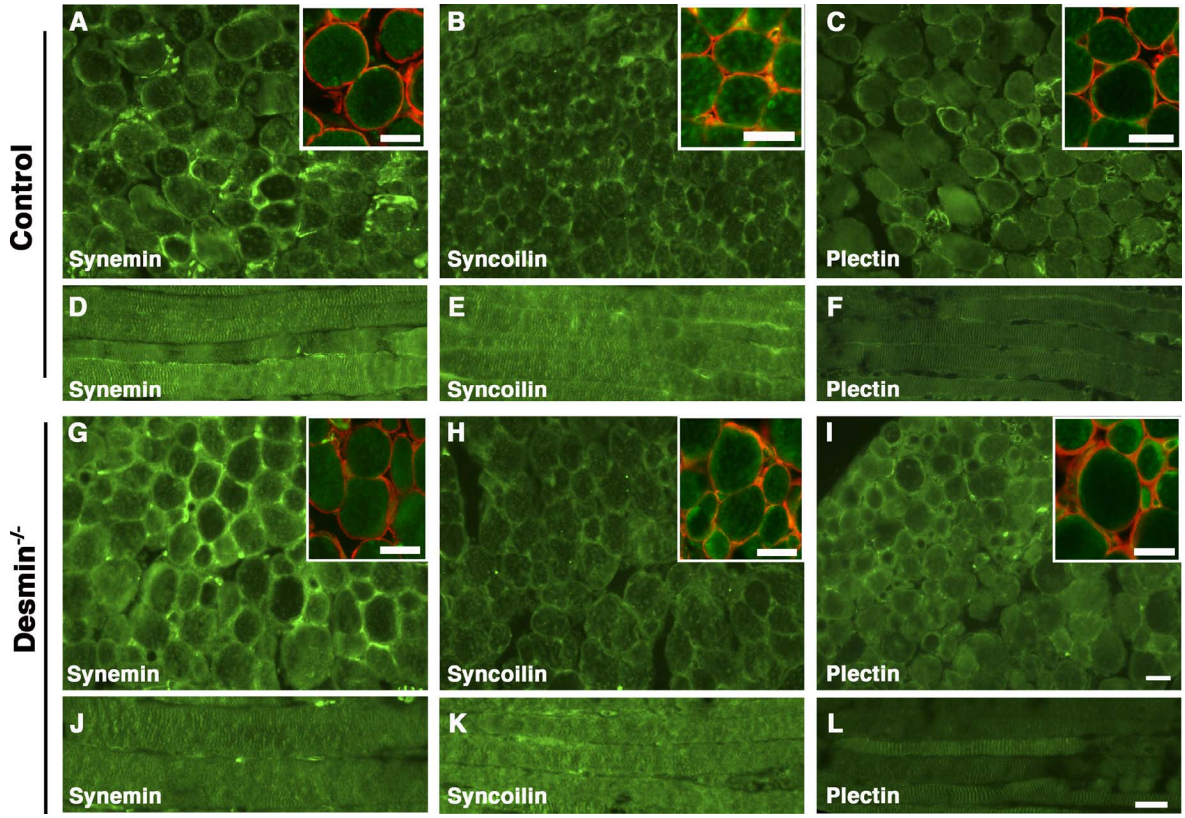

FIGURE 4. Serial cross (**A**–**C**, **G**–**I**) and longitudinal (**D**–**F**, **J**–**L**) sections of EOMs from 1-year old control (**A**–**F**) and desmin$^{-/-}$ (**G**–**L**) mice were immunostained for synemin (**A**, **D**, **G**, **J**), syncoilin (**B**, **E**, **H**, **K**), and plectin (**C**, **F**, **I**, **L**) proteins. All three proteins showed a preserved distribution and labeling intensity in desmin$^{-/-}$ mice characterized by strong subsarcolemmal labeling and mild and variable sarcoplasma labeling with a cross-striated pattern at the Z-discs in longitudinally cut fibers (**J**–**L**). Muscle fibers double-labeled with antibodies against laminin and each of the desmin-binding proteins are shown at higher magnification in the inserts on the *upper right corner*. *Scale bar*: 20 μm.

Investigative Ophthalmology & Visual Science

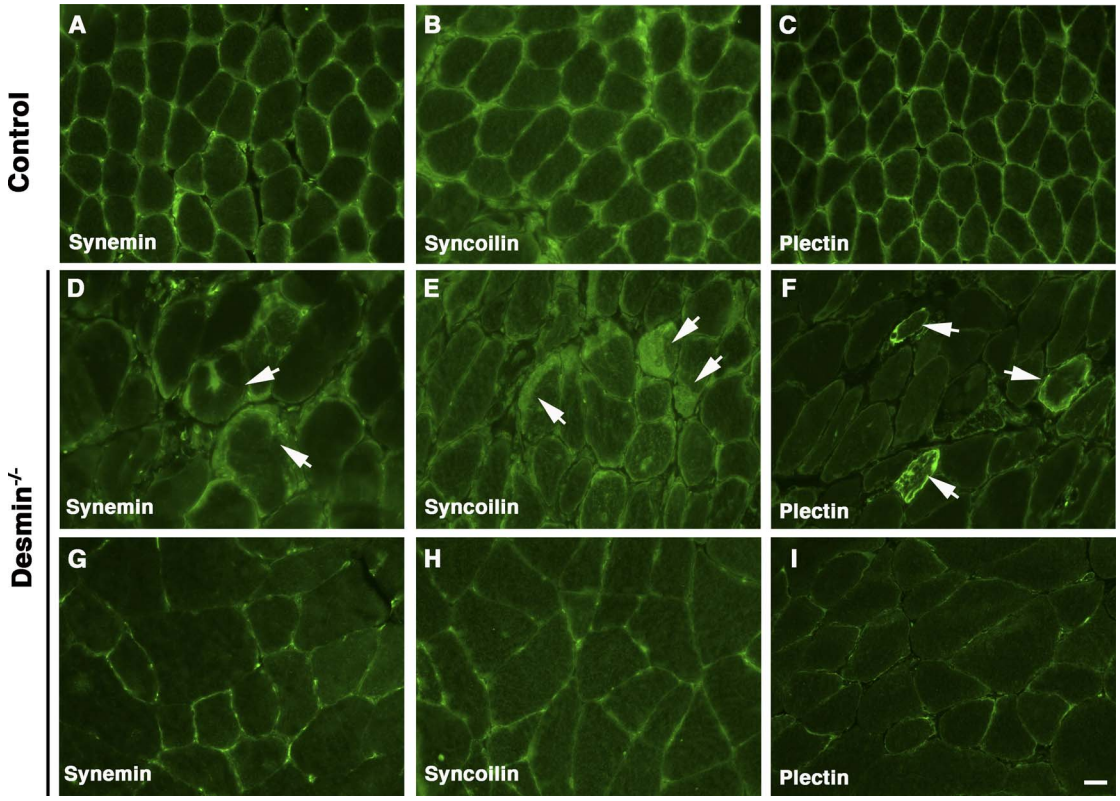

FIGURE 5. Cross sections of soleus (**A–F**) and gastrocnemius muscles (**G–I**) from 1-year-old control (**A–C**) and desmin$^{-/-}$ (**D–I**) mice were immunostained for synemin (**A**, **D**, **G**), syncoilin (**B**, **E**, **H**), and plectin (**C**, **F**, **I**) proteins. All three proteins showed an altered distribution in the soleus muscle of desmin$^{-/-}$ mice with subcellular aggregates accumulated mainly in the subsarcolemmal area (**D–F**, *arrows*), whereas no aggregates were detected on gastrocnemius muscles treated with antibodies against synemin, syncoilin, and plectin (**G–I**). *Scale bar*: 20 μm.

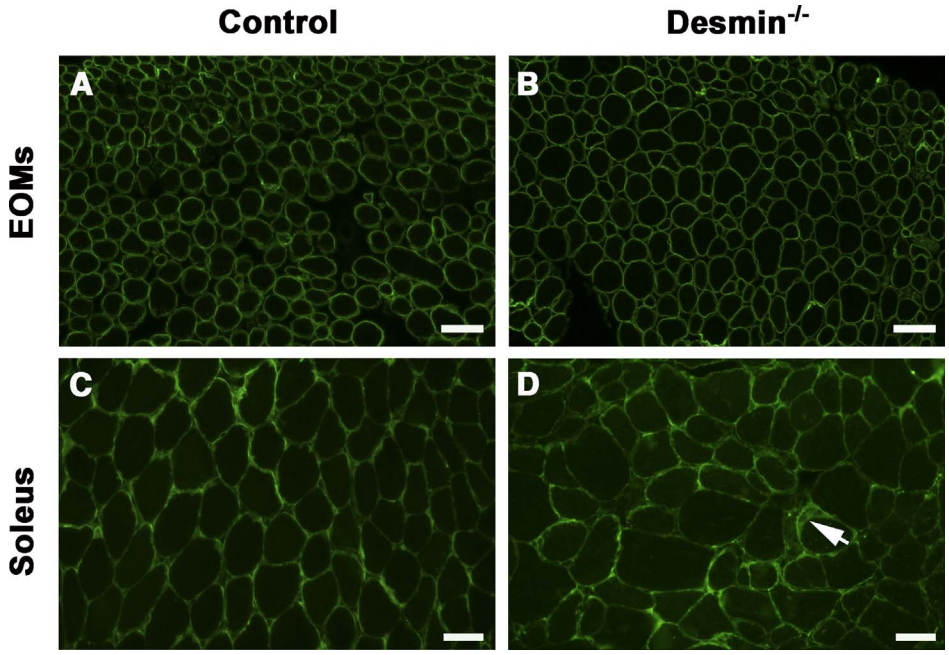

FIGURE 6. Cross-sectioned EOMs (**A**, **B**) and soleus muscles (**C**, **D**) from 1-year-old mice immunostained with the antibody against dystrophin. Desmin$^{-/-}$ EOMs fibers (**B**) were uniformly labeled at the subsarcolemmal level in a pattern similar to that of the control EOMs (**A**). In the soleus muscles from desmin$^{-/-}$ mice, dystrophin accumulations at the subsarcolemmal level were identified in some muscle fibers (**D**, *arrow*). *Scale bar*: 40 μm.

Investigative Ophthalmology & Visual Science

localization of SDH activity in sporadic muscle fibers but similar to those observed in the soleus muscles analyzed and as previously described.[26] We found subsarcolemmal mitochondrial aggregations observed as subsarcolemmal increase in SDH staining in sporadic EOM fibers of approximately half of the animals studied, indicating a disturbed mitochondrial distribution in such muscle fibers. Since desmin is known to interact with mitochondria to provide their correct positioning and, probably, to sustain their function,[13,34] these results suggest that desmin lacking in the EOMs produces detachment and misalignment of mitochondria, observed as mitochondrial aggregates. Previous studies have identified the protein plectin to be responsible for the link between desmin and mitochondria, specifically the isoform 1b of plectin.[27,35] We analyzed plectin distribution in longitudinal and cross-sectioned EOM samples with an antibody that binds to all plectin isoforms, and we found no alterations at the sarcolemma or Z-disc level. Furthermore, no plectin aggregates were detected inside the muscle fibers in the EOMs, despite their presence in the soleus muscle at subsarcolemma level, a location that can correlate with the mitochondrial aggregates revealed by SDH staining.

We further studied the effect of lack of desmin on two additional binding partners, synemin and syncoilin. For both proteins, the distribution and labeling intensity in desmin$^{-/-}$ EOMs were indistinguishable from the pattern of control EOMs. In fact, longitudinal sections immunostained for synemin and syncoilin confirmed their presence along the muscle fiber at the Z-discs despite the lack of desmin in the EOMs. These results contrast with those obtained in the soleus muscle, where synemin and syncoilin subsarcolemmal aggregates were detected, indicating inappropriate protein localization, and were in line with results from gastrocnemius muscle, where no desmin-binding protein aggregates were found. Similarly, previous studies performed on limb muscle of mice lacking desmin also show alterations in synemin[19] and syncoilin,[28] mainly affecting Z-disc location of these proteins and to a lower degree also in the subsarcolemmal area. It seems therefore that desmin is partly necessary for the correct spatial positioning of synemin and syncoilin in skeletal muscle, specifically in the soleus muscle, but not in the EOMs, where synemin and syncoilin maintained their location at the Z-discs and subsarcolemma in spite of the lack of desmin. One possible explanation for these findings would be upregulation of one or more proteins binding to synemin and/or syncoilin that can compensate for the lack of desmin. Recent work from our laboratory demonstrated that nestin expression in adult human EOMs is not restricted to NMJ and MTJ, as it occurs in limb muscle,[21] but that it is present in a high proportion of normal muscle fibers.[10] However, here we could not detect nestin in the EOMs of control or desmin$^{-/-}$ mice, indicating differences between species and that nestin does not substitute for the lack of desmin. The latter is in line with findings in the limb muscles of desmin$^{-/-}$ mice, where the lack of desmin is not compensated for by nestin.[10]

Previous data from studies on desmin$^{-/-}$ mice have shown that highly active muscles, such as the soleus, the tongue, and the diaphragm muscles, are the most affected, whereas the morphology of gastrocnemius muscle is substantially preserved.[24,26] Here we demonstrated that the EOMs, in spite of being very highly active muscles, remain morphologically rather unaffected despite the lack of desmin. The soleus muscle, used in the present study as a positive control of the effects of lack of desmin, contains almost exclusively slow muscle fibers in contrast to the gastrocnemius muscle, which mainly contains fast fibers, similar to the EOMs. Curiously, and in agreement with previous studies,[26] some of the main pathological findings in the gastrocnemius muscle found in our study, such as mitochondrial alterations, seem to preferably occur in the deep portion of the muscle where both fast and slow muscle fibers are present, rather than in those areas entirely composed of fast muscle fibers. Moreover, our study showed that EOMs from desmin$^{-/-}$ mice showed a tendency ($P = 0.06$) to increase the amount of slow fibers in the midbelly region, whereas the total amount of muscle fibers containing MyHCIIa and MyHCIIb was very similar to that of the controls. There were no signs of ongoing degeneration and regeneration in the EOMs from desmin$^{-/-}$ mice; hence we do not attribute these changes in myosin content to degeneration and regeneration. The contrary has been observed in soleus and diaphragm muscles from desmin$^{-/-}$ mice,[24] where degeneration and regeneration processes take place, and decreases in fast fiber content were accompanied by a mild increase in the number of slow muscle fibers, even in younger mice.[24]

Data collected in this study indicate the unique capacity of the EOMs to maintain their cytoarchitecture with adequate localization of the important desmin-binding proteins plectin, synemin, and syncoilin when desmin is completely lacking, in contrast to soleus and gastrocnemius muscles, which appear affected to different degrees. Since we identified some mitochondrial alterations in the EOMs, we suggest that the EOMs have a superior capacity to adapt, but do not completely prevent the effect of lack of desmin. These findings need to be further investigated with complementary high-resolution techniques, such as electron microscopy, in order to more fully characterize the mitochondrial alterations. Furthermore, functional studies to measure mitochondrial respiratory capacity of the EOMs lacking desmin would also be helpful in order to elucidate the consequences of the changes on mitochondria content and localization. Although the EOMs contain a high amount of mitochondria compared to the limb muscles, a lower respiratory capacity has been described in the EOMs.[36] This has been related to a lower content or activity of some mitochondrial electron transport complexes along with a higher content of other complexes, suggesting that the disparity between mitochondrial activity and complex content is likely due to the expression of specific isoforms of electron chain complexes on the EOMs.[36]

In conclusion, the EOMs appeared rather spared in desmin$^{-/-}$ mice, and there was no evidence that the lack of desmin is compensated for by nestin or vimentin or leads to changes in the patterns of distribution of the desmin-binding proteins synemin, syncoilin, or plectin. Further studies are needed in order to elucidate the adaptive mechanisms involved.

Acknowledgments

The authors thank Anna-Karin Olofsson and Mona Lindström for very helpful technical assistance and advice.

Supported by grants from the Swedish Research Council (2015-02438; Stockholm, Sweden), County Council of Västerbotten (Umeå, Sweden), Ögonfonden (Umeå, Sweden), and Kronprinsessan Margaretas Arbetsnämnd för Synskadade (Valdemarsvik, Sweden).

Disclosure: **M.A. Rodríguez**, None; **J.-X. Liu**, None; **K. Parkkonen**, None; **Z. Li**, None; **F. Pedrosa Domellöf**, None

References

1. Fischer MD, Budak MT, Bakay M, et al. Definition of the unique human extraocular muscle allotype by expression profiling. *Physiol Genomics*. 2005;22:283–291.
2. McLoon LK, Christiansen SP. Extraocular muscles: extraocular muscle anatomy. In: Dartt DA, Besharse JC, Dana R, eds. *Encyclopedia of the Eye*. Vol 2. Oxford: Academic Press; 2010:89–98.

3. Kaminski HJ, Al-Hakim M, Leigh RJ, Bashar MK, Ruff RL. Extraocular muscles are spared in advanced Duchenne dystrophy. *Ann Neurol*. 1992;32:586–588.
4. Khurana TS, Prendergast RA, Alameddine HS, et al. Absence of extraocular muscle pathology in Duchenne's muscular dystrophy: role for calcium homeostasis in extraocular muscle sparing. *J Exp Med*. 1995;182:467–475.
5. Nyström A, Holmblad J, Pedrosa-Domellöf F, Sasaki T, Durbeej M. Extraocular muscle is spared upon complete laminin α2 chain deficiency: comparative expression of laminin and integrin isoforms. *Matrix Biol*. 2006;25:382–385.
6. Ahmadi M, Liu J-X, Brännström T, Andersen PM, Stål P, Pedrosa-Domellöf F. Human extraocular muscles in ALS. *Invest Ophthalmol Vis Sci*. 2010;51:3494–3501.
7. Clemen CS, Herrmann H, Strelkov SV, Schröder R. Desminopathies: pathology and mechanisms. *Acta Neuropathol*. 2013; 125:47–75.
8. van Spaendonck-Zwarts K, van Hessem L, Jongbloed J, et al. Desmin-related myopathy. *Clin Genet*. 2011;80:354–366.
9. Li ZL, Lilienbaum A, Butler-Browne G, Paulin D. Human desmin-coding gene: complete nucleotide sequence, characterization and regulation of expression during myogenesis and development. *Gene*. 1989;78:243–254.
10. Janbaz AH, Lindström M, Liu J-X, Pedrosa Domellöf F. Intermediate filaments in the human extraocular muscles. *Invest Ophthalmol Vis Sci*. 2014;55:5151–5159.
11. Li Z, Colucci-Guyon E, Pinçon-Raymond M, et al. Cardiovascular lesions and skeletal myopathy in mice lacking desmin. *Dev Biol*. 1996;175:362–366.
12. Capetanaki Y, Milner DJ, Weitzer G. Desmin muscle formation and maintenance: knockouts and consequences. *Cell Struct Funct*. 1997;22:103–116.
13. Reipert S, Steinböck F, Fischer I, Bittner RE, Zeöld A, Wiche G. Association of mitochondria with plectin and desmin intermediate filaments in striated muscle. *Exp Cell Res*. 1999;252:479–491.
14. Kim S, Coulombe PA. Intermediate filament scaffolds fulfill mechanical, organizational, and signaling functions in the cytoplasm. *Genes Dev*. 2007;21:1581–1597.
15. Toivola DM, Tao G-Z, Habtezion A, Liao J, Omary MB. Cellular integrity plus: organelle-related and protein-targeting functions of intermediate filaments. *Trends Cell Biol*. 2005;15: 608–617.
16. Bellin RM, Sernett SW, Becker B, Ip W, Huiatt TW, Robson RM. Molecular characteristics and interactions of the intermediate filament protein synemin. Interactions with alpha-actinin may anchor synemin-containing heterofilaments. *J Biol Chem*. 1999;274:29493–29499.
17. Poon E, Howman EV, Newey SE, Davies KE. Association of syncoilin and desmin: linking intermediate filament proteins to the dystrophin-associated protein complex. *J Biol Chem*. 2002;277:3433–3439.
18. Bellin RM, Huiatt TW, Critchley DR, Robson RM. Synemin may function to directly link muscle cell intermediate filaments to both myofibrillar Z-lines and costameres. *J Biol Chem*. 2001; 276:32330–32337.
19. Carlsson L, Li ZL, Paulin D, et al. Differences in the distribution of synemin, paranemin, and plectin in skeletal muscles of wild-type and desmin knock-out mice. *Histochem Cell Biol*. 2000;114:39–47.
20. Newey SE, Howman EV, Ponting CP, et al. Syncoilin, a novel member of the intermediate filament superfamily that interacts with α-dystrobrevin in skeletal muscle. *J Biol Chem*. 2001;276:6645–6655.
21. Carlsson L, Li Z, Paulin D, Thornell L-E. Nestin is expressed during development and in myotendinous and neuromuscular junctions in wild type and desmin knock-out mice. *Exp Cell Res*. 1999;251:213–223.
22. Sjöberg G, Jiang WQ, Ringertz NR, Lendahl U, Sejersen T. Colocalization of nestin and vimentin/desmin in skeletal muscle cells demonstrated by three-dimensional fluorescence digital imaging microscopy. *Exp Cell Res*. 1994;214:447–458.
23. Vaittinen S, Lukka R, Sahlgren C, et al. The expression of intermediate filament protein nestin as related to vimentin and desmin in regenerating skeletal muscle. *J Neuropathol Exp Neurol*. 2001;60:588–597.
24. Li Z, Mericskay M, Agbulut O, et al. Desmin is essential for the tensile strength and integrity of myofibrils but not for myogenic commitment, differentiation, and fusion of skeletal muscle. *J Cell Biol*. 1997;139:129–144.
25. Milner DJ, Weitzer G, Tran D, Bradley A, Capetanaki Y. Disruption of muscle architecture and myocardial degeneration in mice lacking desmin. *J Cell Biol*. 1996;134:1255–1270.
26. Milner DJ, Mavroidis M, Weisleder N, Capetanaki Y. Desmin cytoskeleton linked to muscle mitochondrial distribution and respiratory function. *J Cell Biol*. 2000;150:1283–1298.
27. Winter L, Abrahamsberg C, Wiche G. Plectin isoform 1b mediates mitochondrion–intermediate filament network linkage and controls organelle shape. *J Cell Biol*. 2008;181:903–911.
28. McCullagh KJA, Edwards B, Poon E, Lovering RM, Paulin D, Davies KE. Intermediate filament-like protein syncoilin in normal and myopathic striated muscle. *Neuromuscul Disord*. 2007;17:970–979.
29. Clemen CS, Stöckigt F, Strucksberg K-H, et al. The toxic effect of R350P mutant desmin in striated muscle of man and mouse. *Acta Neuropathol*. 2015;129:297–315.
30. Bär H, Fischer D, Goudeau B, et al. Pathogenic effects of a novel heterozygous R350P desmin mutation on the assembly of desmin intermediate filaments in vivo and in vitro. *Hum Mol Genet*. 2005;14:1251–1260.
31. Fountoulakis M, Soumaka E, Rapti K, et al. Alterations in the heart mitochondrial proteome in a desmin null heart failure model. *J Mol Cell Cardiol*. 2005;38:461–474.
32. Dubowitz V, Sewry CA, Oldfors A, Lane RJM. *Muscle Biopsy: A Practical Approach*. Saunders; 2013:21–24.
33. Schindelin J, Arganda-Carreras I, Frise E, et al. Fiji: an open-source platform for biological-image analysis. *Nat Methods*. 2012;9:676–682.
34. Winter L, Kuznetsov AV, Grimm M, Zeöld A, Fischer I, Wiche G. Plectin isoform P1b and P1d deficiencies differentially affect mitochondrial morphology and function in skeletal muscle. *Hum Mol Genet*. 2015;24:4530–4544.
35. Konieczny P, Fuchs P, Reipert S, et al. Myofiber integrity depends on desmin network targeting to Z-disks and costameres via distinct plectin isoforms. *J Cell Biol*. 2008; 181:667–681.
36. Patel SP, Gamboa JL, McMullen CA, Rabchevsky A, Andrade FH. Lower respiratory capacity in extraocular muscle mitochondria: evidence for intrinsic differences in mitochondrial composition and function. *Invest Ophthalmol Vis Sci*. 2009;50:180–186.

Investigative Ophthalmology & Visual Science